

Research Article

# Mechanism of Action of Curcumin for Rheumatoid Arthritis Based on Machine Learning, Molecular Dynamics and Cellular Experiments

Jianwei Xiao , Xinmin Huang , Xu Cai , Yiwei Hong , Zhenbo Yan ,  
Xinpeng Chen\* 

Department of Rheumatology and Immunology, Shenzhen Futian Hospital for Rheumatic Diseases, Shenzhen, China

## Abstract

**Objective:** Curcumin has been widely used in rheumatoid arthritis (RA) treatment and the previous study also proved its effectiveness. However, the pharmacological mechanism is still not clear. The current study intends to discuss the potential mechanism of action of curcumin in RA treatment through machine learning, network pharmacology, molecular dynamics and cellular experiments. **Methods:** RA-related microarray data were obtained from three GEO datasets: GSE55235, GSE55457 and GSE77298. Machine learning methods including XGBOOST, LASSO and SVM were adopted to screen out potential targets of RA pathogenesis. Online tools SwissTargetPrediction and Similarity ensemble approach were visited to predict potential targets of action of curcumin. The key target was identified via a Venn diagram and processed for molecular docking and molecular dynamics simulation with curcumin. Fibroblast-like synoviocytes (RA-FLSs) were selected to study the effect of curcumin at different concentrations (20, 40 and 80  $\mu\text{mol/L}$ ) on cell proliferation and apoptosis using MTT and flow cytometry assays. In addition, Western blot was used to examine the protein level. **Results:** Arachidonate 5-Lipoxygenase (ALOX5) was identified as a key target of RA following bioinformatics prediction. Results of molecular docking and molecular dynamics simulation demonstrated the tight binding between curcumin and ALOX5 with stable function. RA-FLSs intervened with different concentrations of curcumin (20, 40 and 80  $\mu\text{mol/L}$ ) exhibited decreased potential in proliferation while increased apoptosis, which were in a dose-dependent manner. Additionally, with the increase of curcumin concentration, the protein level of ALOX5 gradually decreased. **Conclusion:** Curcumin may exert its therapeutic effects in RA treatment via down-regulating the expression of ALOX5.

## Keywords

Rheumatoid Arthritis, Molecular Docking, Molecular Dynamics, Curcumin, ALOX5

## 1. Introduction

Rheumatoid arthritis (RA) is a chronic autoimmune inflammatory disease identified by irreversible cartilage damage and secondary bony erosion. The lesions progress over time,

resulting in progressive synovial joint damage and various extra-articular manifestations [1]. Interleukin-1  $\beta$  (IL-1 $\beta$ ) and tumor necrosis factor - $\alpha$  (TNF- $\alpha$ ) are common inflammatory

\*Corresponding author: chenxinpeng0517@163.com (Xinpeng Chen)

Received: 6 May 2024; Accepted: 31 May 2024; Published: 13 June 2024



Copyright: © The Author(s), 2024. Published by Science Publishing Group. This is an **Open Access** article, distributed under the terms of the Creative Commons Attribution 4.0 License (<http://creativecommons.org/licenses/by/4.0/>), which permits unrestricted use, distribution and reproduction in any medium, provided the original work is properly cited.

cytokines critical in the course of chronic synovial diseases [2]. Except the common inflammatory cytokines, 5-lipoxygenase (ALOX5) was also reported as a participant in the progression of inflammation with up-regulated expression in RA synovial tissues [3]. As a rate-limiting enzyme, ALOX5 is responsible for leukotriene (LTs) biosynthesis. LTs are major inflammatory mediators that can regulate the expression of TNF- $\alpha$  and IL-1 $\beta$  via activating and recruiting inflammatory cells and immune effector cells in the presence of RA, thereby advancing the differentiation of osteoclasts [4]. At present, ALOX5 has been used as a novel target of inflammation in treatment of a variety of diseases.

Currently, therapy targeting inflammatory factors comprises the majority of pharmaceutical treatments for RA. Etanercept and Infliximab, for example, are common agents but always accompanied by some side effects [5]. To obtain a safer profile, more scholars shift their attention to natural products. Curcumin extracted from *Curcuma longa* (turmeric) is one of the various natural products and was reported as a potential effective drug for RA [6, 7]. In this study, ALOX5 was identified as a crucial target in RA pathogenesis through machine learning approaches. The potential mechanism of action of curcumin in RA treatment was investigated via molecular docking, molecular dynamics simulations, and cellular experiments. This study aimed at providing theoretical basis for curcumin application in RA treatment.

## 2. Materials and Methods

### 2.1. Data Acquisition and Merging

The key word search using the word “Rheumatoid Arthritis” in Gene Expression Omnibus (GEO) database identified three datasets GSE55235, GSE55457 and GSE77298 with synovial tissues as research subjects. Microarray data of GSE55235 (Normal, n=10; RA, n=10) and GSE55457 (Normal, n=10; RA, n=13) were generated using GPL96, while that of GSE77298 (Normal, n=7; RA, n=16) was generated using GPL570. The three datasets were merged and batch-corrected using the packages Limma and SVA of RStudio v3.53, and the batch effect was assessed with principal component analysis (PCA).

### 2.2. Acquisition of Potential Target Genes Critical to RA Pathogenesis

Multiple machine learning methods were adopted to analyze potential target genes critical to RA pathogenesis from the annotated gene sets. The LASSO algorithm was adopted using the R package glmnet. The XGBOOST method was applied with eta =0.3, nround=1000 using the R package XGBOOST. Support vector machine (SVM) was employed with the C penalty parameter set as 0.1 and the kernel function as radial basis function using the R package randomFores.

Results of the three models were mapped to a Venn diagram to obtain the potential target genes.

### 2.3. Prediction of Target Genes of Curcumin and Acquisition of Targets for RA Treatment

The molecular structure of curcumin in the SMILES format was uploaded to the online databases *SwissTarget Prediction* [8] and *Similarity ensemble approach* [9] to predict the targets of curcumin. The *SwissTargetPrediction* database includes 370,000 known active substances and *Similarity ensemble approach* quantitatively groups and establishes related proteins based on the chemical similarity of their ligands. For *SwissTargetPrediction*, the genes with probability greater than 0.1 were selected, while for *Similarity ensemble approach*, the genes with maximum Tanimoto Coefficient (MaxTC) greater than 0.5 were selected. A Venn diagram was plotted to obtain the potential target genes of curcumin.

The results of step 1.2 and step 1.3 were mapped to a Venn diagram to obtain the potential targets of curcumin for RA therapy.

### 2.4. Molecular Docking and Molecular Dynamics Simulation

The 3D structure of target proteins were downloaded from the RCSB PDB database and uploaded to *Playmolecule* [10] to predict the docking pocket. The molecular structure of curcumin obtained from the Pubchem database was imported into the ChemBio3D Ultra 14.0 to minimize its energy. The coordinates of the binding sites with the highest score predicted by *Playmolecule* were imported into AutoDock Tools 1.5.6 software. Molecular docking calculations were completed using the AutoDock Vina 1.1.2 and the ligands with the lowest binding energy were selected as the optimal ligands.

Molecular dynamics simulation was performed using Gromacs 2019.5 software. Molecular coordinate files (Gro format) of the active small molecules and proteins were created by the ATB website [11] and Gromacs respectively. Topology files were then generated. Gromos54a7\_atb force field and SPC water molecule model were selected, and the system charges were neutralized. The system was simulated at 300 K after optimization for molecular mechanics using the steepest descent method. Equilibrium for NVT and NPT ensembles was achieved and simulations were run for 20 ns. The binding free energy of ligand to receptor was calculated through g\_mmpbsa [12]. Changes in the binding positions and the hydrogen bonds before and after the simulation were compared, and the root mean square deviation (RMSD) of the protein-small molecule complex, radius of gyration (Rg) of proteins and solvent-accessible surface area (SASA) were evaluated. The plausibility of simulated protein structure was evaluated via the Ramachandran map.

## 2.5. Cell Experiment Materials

The RA fibroblast-like synoviocytes (RA-FLSs) derived from ATCC. Dulbecco's modified Eagle's medium, fetal bovine serum (FBS) and trypsin were purchased from GIBCO company. Curcumin, MTT reagent, dimethyl sulfoxide (DMSO) and penicillin-streptomycin were ordered from sigma-Aldrich company. Annexin V-FITC/PI cell apoptosis detection kit was purchased from Shanghai Absin Bioscience Inc. BCA protein assay kit and RIPA lysis buffer were obtained from Beijing Solarbio Life sciences Inc. Polyvinylidene fluoride (PVDF) films and ECL hypersensitive chemoluminescent solution were purchased from Millipore (USA). Primary rabbit-anti-human ALOX5, rabbit-anti-human  $\beta$ -actin and secondary horseradish peroxidase (HRP)-conjugated goat anti-rabbit IgG were purchased from Abcam (USA). Microplate reader was derived from BioTek (USA), flow cytometry was from BD (USA), and Gel Imaging System was from Shanghai Tanon company.

## 2.6. Cell Culture and Drug Preparation

RA-FLSs were cultured in the DMEM containing 10% FBS, 100 U/mL penicillin and 100  $\mu$ g/mL streptomycin, placed in a 37 °C incubator with 5% CO<sub>2</sub>. Experimental Curcumin solution was prepared by dissolution in trace amounts of DMSO solution and dilution with DMEM, and the final concentration of DMSO was kept below 0.1%.

## 2.7. MTT Assay and Annexin V-FITC/PI Double Staining Assay

RA-FLSs in the logarithmic growth phase were digested, harvested and counted. The cells were then seeded in a 96-well plate at  $1 \times 10^4$  cells/well. Upon 80-90% confluency, the cells were intervened with curcumin solution (20, 40 and 80  $\mu$ mol/L) or curcumin-free DMSO for 48 h. After that, 20  $\mu$ L MTT reagent (5 mg/mL) was added into each well and the cells were continuously cultured for 4 h. The supernatant was removed. Each well was added with 150  $\mu$ L DMSO to dissolve the crystal products. Optical density at 490 nm (OD490) was read with a microplate reader to calculate the proliferation rate.

Following the grouping method of in step 1.7.3, RA-FLSs were digested, collected and washed twice with phosphate

buffered saline (PBS). The cells were then resuspended by  $1 \times$  Annexin V binding buffer and mixed with 10  $\mu$ L Annexin V-FITC and 10  $\mu$ L PI solutions. Cell apoptosis was determined by flow cytometry after 20 min of reaction in the dark.

## 2.8. Western Blot

Cell proteins were extracted with RIPA lysis buffer and the concentrations were determined with BCA Protein Assay Kit. Protein lysates (50  $\mu$ g) were denatured at 100 °C for 10 min with equal amounts of loading buffer (1:1) and then separated by SDS-PAGE. The separated proteins were wet-transferred to a PVDF membrane, which was subsequently blocked in 5% skim milk powder for 2h at room temperature. Antibody-antigen reactions were realized by addition of primary antibodies at 4 °C overnight, followed by hybridization with the HRP-conjugated secondary antibodies at room temperature for 2h. The membrane was washed three times with TBST for 10 min each time before and after the hybridization. The membrane was exposed to ECL hypersensitive chemiluminescent solution and protein bands were developed on the Gel Imaging System. Grey values of the bands were measured by Image-J software. The protein level of ALOX5 relative to  $\beta$ -actin was calculated.

## 2.9. Statistical Analysis

The data were presented as mean value  $\pm$  S. D. (standard deviation). One-way ANOVA analysis was used for multiple-group comparisons, with  $P < 0.05$  considered to be statistically significant. Data processing of the study was performed using the GraphPad Prism 9.0 software.

## 3. Results

### 3.1. Data Merging and Batch Correction

Following data merging and batch correlation, totally 39 RA tissue samples and 27 normal tissue samples were obtained from the GSE55235, GSE55457 and GSE77298 three datasets. Raw data were processed for PCA, exhibiting significant difference across the three datasets while random distribution after background correction and normalization, which suggested distinct batch effect (Figure 1).

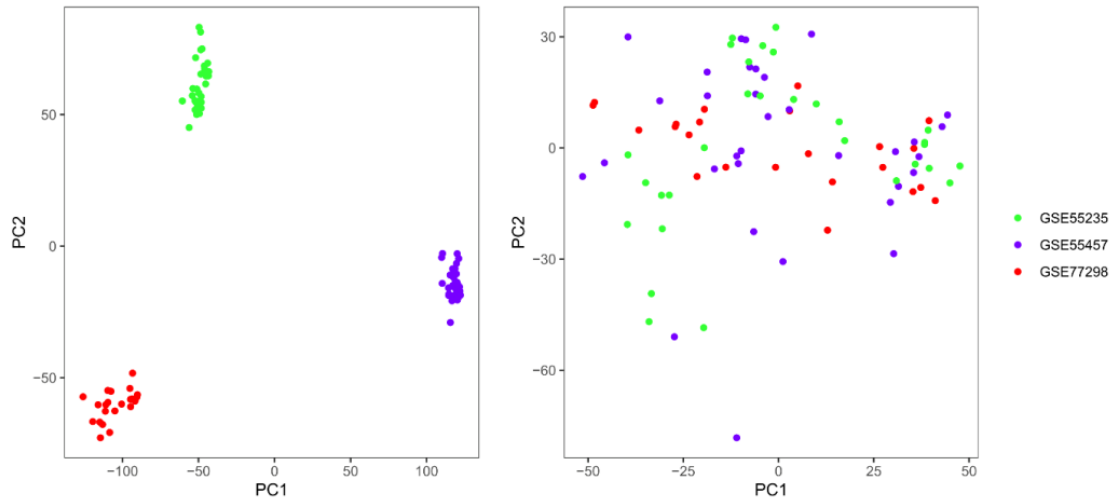


Figure 1. PCA plots before (Left) and after (Right) data background correction and normalization.

### 3.2. Acquisition of Potential Target Genes Critical to RA Pathogenesis

LASSO, SVM and XGBOOST algorithms identified 24, 48 and 41 key targets of RA pathogenesis, respectively. Two common targets were obtained, including GABARAPL1 and ALOX5 (Figure 2).

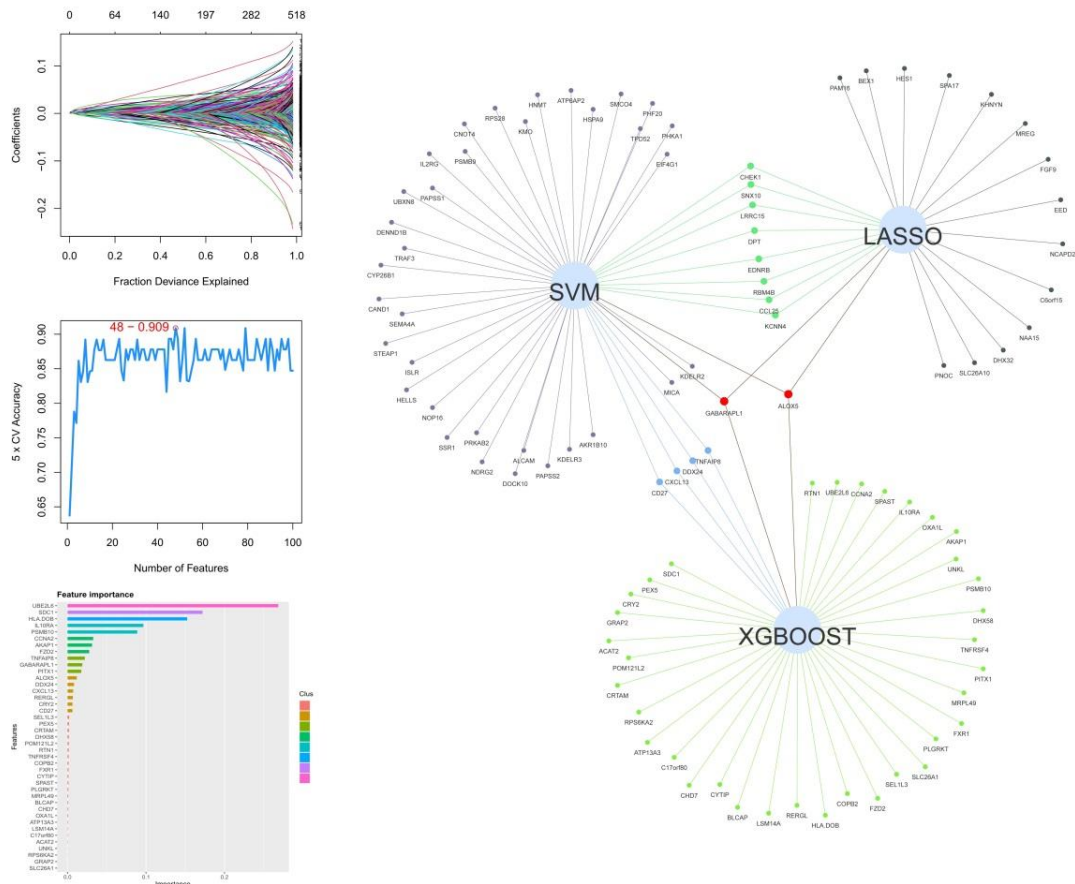
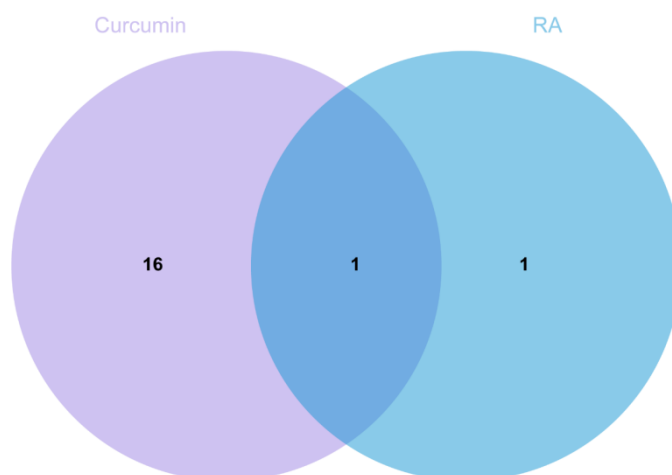


Figure 2. Venn diagram of the machine learning results of LASSO, XGBOOST and SVM (two common targets, GABARAPL1 and ALOX5, were obtained).

### 3.3. Acquisition of Potential Targets Critical to RA Pathogenesis and Curcumin Treatment

Prediction of targets of curcumin from *SwissTargetPrediction* and *Similarity ensemble approach* respectively ob-

tained 67 and 28 potential target proteins, among which 17 targets were overlapped. Furthermore, there was only one target termed ALOX5 potentially associated with RA pathogenesis and curcumin treatment (Figure 3).



**Figure 3.** Venn diagram of targets of RA pathogenesis and curcumin treatment (one common target termed ALOX5 was identified).

### 3.4. Molecular Docking

Three small-molecule docking pockets of ALOX5 protein were predicted by *Playmolecule*, and the coordinate for the pocket with the highest score was (X=-0.7, Y= -94.6, Z=

-51.1). The binding energy between curcumin and ALOX5 protein was -8.8 kcal mol<sup>-1</sup> (binding energy < -5 kcal mol<sup>-1</sup> indicates strong binding activity). Results showed that curcumin formed multiple hydrogen bonds and hydrophobic bonds with ALOX5 protein, presenting strong binding ability between curcumin and ALOX5 protein (Figure 4).

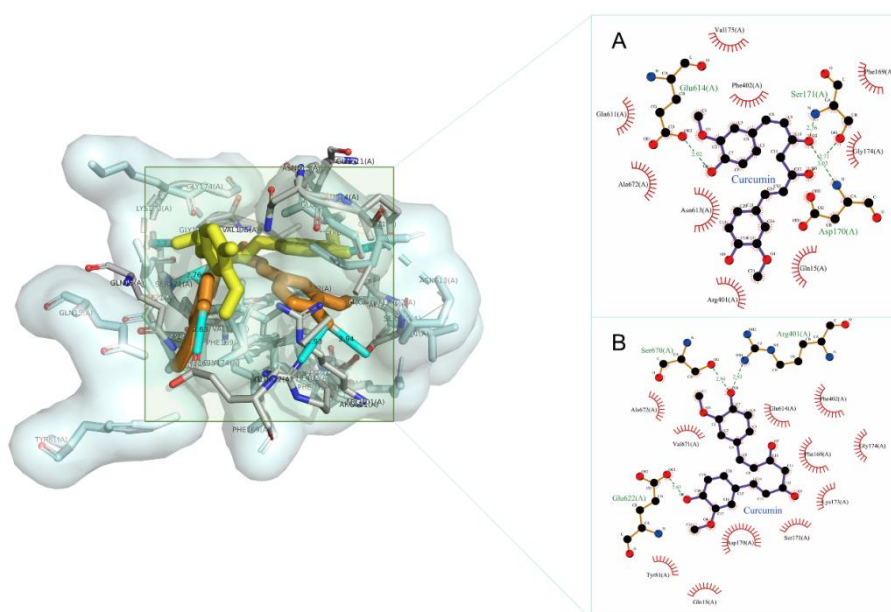


**Figure 4.** Molecular docking results before and after the molecular dynamics simulation (Left: the yellow represents the position before simulation and the orange represents the position after simulation. Right: A: The molecular docking results before simulation; B: The molecular docking results after simulation).

### 3.5. Molecular Dynamics Simulation

The RMSD of the complex comprised of curcumin and ALOX5 protein reached equilibrium at around 10 ns, with a fluctuation value less than 0.05 nm. The Rg decreased gradually with time, demonstrating that the complex structure tended to be stable following binding. In the meantime, the SASA also gradually reduced, suggestive of the gradual stabilization of the whole system with the increase in the hydrophobicity (Figure 5).

The volume of the ALOX5 protein pocket was from 538.277 Å<sup>3</sup> before to 363.044 Å<sup>3</sup> after binding. Hydrogen-bonding interactions in the complex were kept in more than two hydrogen bonds during the whole simulation process.

There was no significant change in position of active small molecule before and after simulation, presenting with stable binding with ALOX5 protein via hydrogen and hydrophobic bonds in the active pockets. The simulated protein structure was evaluated as plausible via the Ramachandran map, with 98.8% amino acid residues being within the reasonable range (Figure 6).

The total binding free energy of curcumin to ALOX5 protein was  $-85.582 \pm 36.460$  kJ/mol. The binding of the two was mainly through van der Waals force ( $-169.733 \pm 12.506$  kJ/mol), electrostatic potential energy ( $-45.259 \pm 12.999$  kJ/mol) and nonpolar solvation energy ( $-20.489 \pm 1.307$  kJ/mol). Polar solvation energy played an inhibitory role in the binding ( $149.899 \pm 32.159$  kJ/mol).

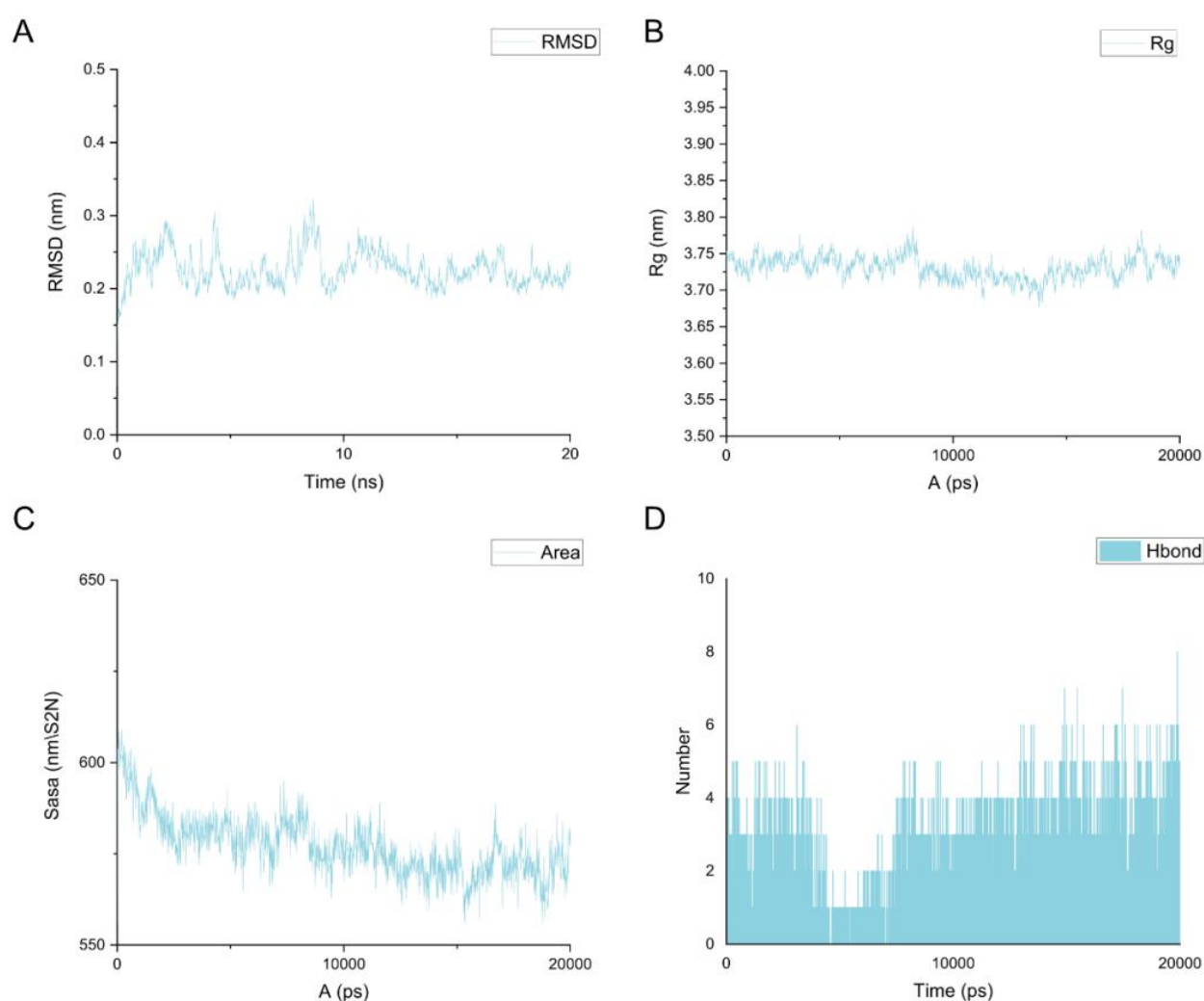


**Figure 5.** The Root Mean Square Deviation (RMSD), solvent-accessible surface (SASA) and hydrogen bonds change of the curcumin-ALOX5 complex. (A-C. The RMSD, protein radius of gyration (Rg) and SASA of the curcumin-ALOX5 complex after 20 ns of simulation. D. The changes in number of hydrogen bonds during the simulation).

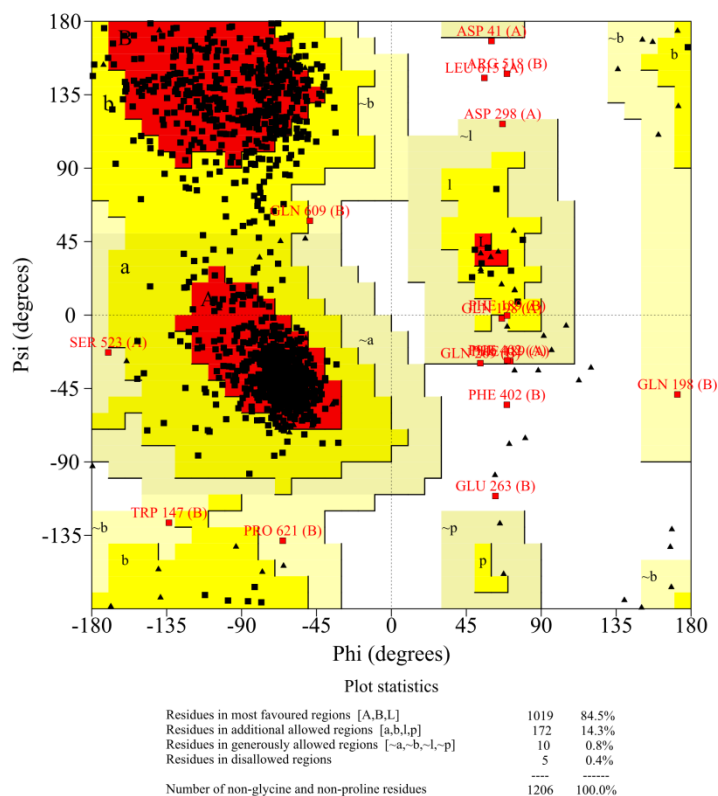


**Figure 6.** The Ramachandran map after simulation (98.8% amino acid residues were in the reasonable range).

### 3.6. Curcumin Inhibits the Proliferation of RA-FLSs

After 48-h intervention with curcumin in different concentrations (20, 40 and 80  $\mu\text{mol/L}$ ) or curcumin-free DMSO, RA-FLSs exhibited significantly decreased potential of proliferation as compared to the control cells ( $p < 0.05$ ), which proved that curcumin could inhibit the proliferation of RA-FLSs (Figure 7).

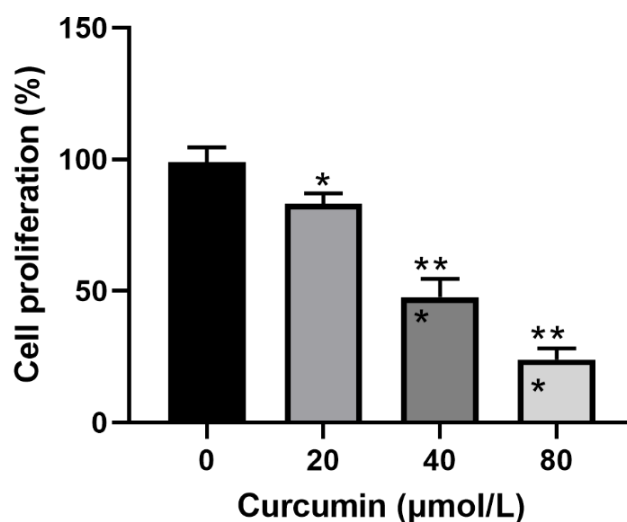


**Figure 7.** Curcumin inhibits the proliferation of RA-FLSs.

### 3.7. Curcumin Induces the Apoptosis of RA-FLSs

Significant increase in the rate of apoptosis in RA-FLSs was demonstrated in the groups with different concentrations of

curcumin as compared to the control group ( $p < 0.05$ ), indicating that curcumin could induce the apoptosis of RA-FLSs (Figure 8).

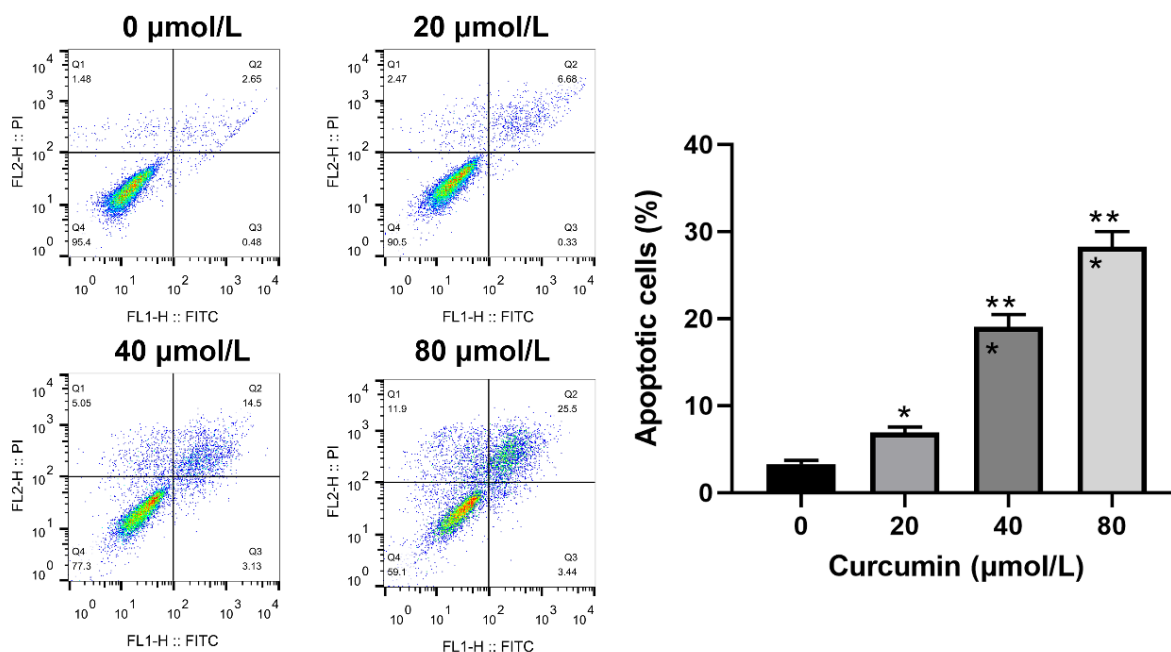


Figure 8. Curcumin induces the apoptosis of RA-FLSs.

### 3.8. Curcumin Reduces the Protein Expression of ALOX5 in RA-FLSs

Protein level of ALOX5 in RA-FLSs was examined and exhibited a distinct downward trend in cells intervened with curcumin at different concentrations, demonstrating that curcumin could down-regulate the expression of ALOX5 proteins in RA-FLSs (Figure 9).

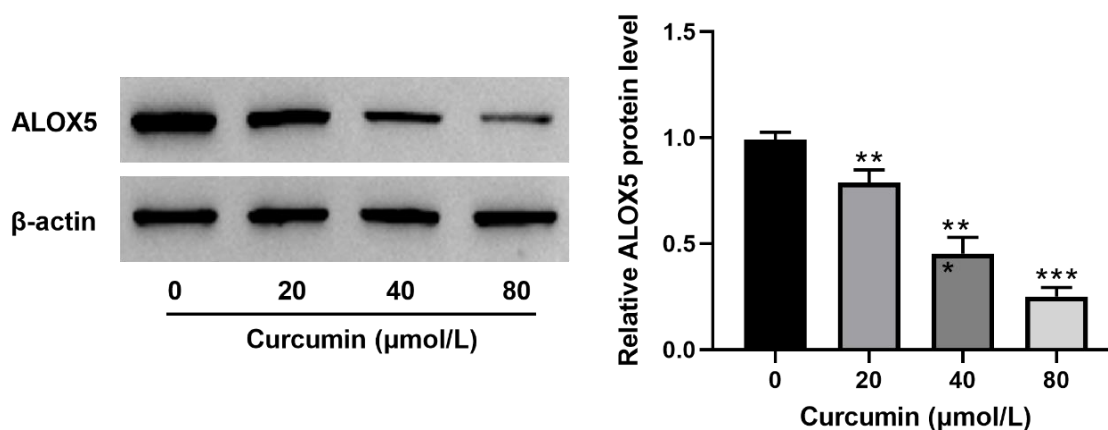


Figure 9. Curcumin decreases ALOX5 protein expression in RA-FLSs.

## 4. Discussion

RA is characterized by synovial hyperplasia majorly caused by enhanced proliferation of FLSs. It has been established that aberrant proliferation of FLSs plays a key role in the patho-

genesis and progression of RA via inducing the production of inflammatory cytokines. Hence, it will be highly significant in RA treatment through inhibiting the proliferation of FLSs, promoting their apoptosis and controlling the level of inflammation. In recent years, biological agents have shown great potential in treatment of RA and has been increasingly

applied in clinic due to its marked efficacy. Nevertheless, the application is greatly limited because of the high price and side effects like infection.

Curcumin is a yellow hydrophobic polyphenol extracted from *Curcuma longa* (turmeric) that has multiple pharmacological activities against a variety of chronic diseases, such as cancer [13, 14], atherosclerosis [15], and Alzheimer's disease [16]. It was reported that curcumin could inhibit the proliferation of RA-FLSs and decrease their capability to secrete TNF- $\alpha$  and interleukin-6 (IL-6) [17]. Few studies have been reported on the relationship between curcumin and ALOX5.

Multiple machine learning techniques were employed in the current study to pinpoint ALOX5 as a key target in RA, utilizing three RA-related GEO datasets. A study proved that the expression of ALOX5 significantly increased in RA synovium, which was positively correlated with the expression levels of pro-inflammatory mediators, IL-1 $\beta$  and TNF- $\alpha$  [18]. Another study also suggested distinct increase in ALOX5 expression in RA synovial biopsy while a significant reduction after glucocorticoids treatment, showing that ALOX5 plays a crucial part in RA inflammation [19].

ALOX5 is a dioxygenase that plays a core part in inflammation via catalyzing the peroxidation of polyunsaturated fatty acids (PUFA). Currently, numerous studies proved that the lipid peroxidation of PUFA involves in the etiologies of a diverse range of pathological conditions, including cancer [20], cardiovascular disease [21] and disease of the nervous system [22]. PUFA contains various straight-chain fatty acids including linoleic acid, eicosapentaenoic acid and arachidonic acid (AA). AA is one of the paramount PUFA in mammalian cells necessary for membrane integrity. Besides, it is also the direct precursor of many bioactive mediators, such as LTs, prostaglandin, thromboxane A<sub>2</sub>, etc. ALOX genes contribute most significantly to the production of lipid peroxides, among the multiple enzymes involved in AA metabolism [23]. In human, ALOX genes have six functional isoforms [24]. ALOX5 is responsible for the biosynthesis of LTs, especially the downstream product leukotriene B<sub>4</sub> (LTB<sub>4</sub>), a potent proinflammatory chemoattractant involved in ALOX5 cascade reactions and considered as an important mediator of joint inflammation in RA [25]. Research found that the serum LTB<sub>4</sub> level in RA patients was higher than that in normal people [26]. Moreover, LTB<sub>4</sub> is also greatly implicated with the pain induction and bone damage [27].

An animal experiment revealed that deficiency of ALOX5 or administration of ALOX5 inhibitor could protect mice from experiencing inflammatory arthritis [28]. Lin et al. [29] reported that the ALOX5 inhibitor MK-886 antagonized the expression and release of TNF- $\alpha$ -induced IL-6 and monocyte chemoattractant protein-1 in RA-FLSs in a dose-dependent manner. Besides, consistent results were demonstrated upon knock-down of ALOX5 via transient transfection with ALOX5 shRNA, suggesting that ALOX5 plays an essential role in the expression of TNF- $\alpha$ -induced cytokines and chemokines in human RA-FLSs. The authors also found that

MK-886 antagonized the activation of IKK $\alpha/\beta$  in RA-FLSs and its effect on I $\kappa$ B $\alpha$  phosphorylation and degradation. This suggested that ALOX5 might be involved in expression of TNF- $\alpha$ -induced cytokines and chemokines through the Nuclear Factor Kappa B (NF- $\kappa$ B) signaling pathway. Based on the studies above, suppressing ALOX5 might be one effective treatment of RA.

Here, results of molecular docking and molecular dynamics simulation suggested the tight binding between curcumin and ALOX5 protein with a low total binding free energy. Additionally, during the whole simulation process, hydrogen-bonding interactions were kept in 1-7 hydrogen bonds in the curcumin-ALOX5 complex and the volume of the protein binding pocket gradually decreased with time, implying the strong binding between curcumin and ALOX5 protein, which was conducive to inhibiting the protein function. Further Ramachandran map proved the plausibility of the simulated protein structure. Moreover, cellular experiments were performed to study the effect of curcumin on proliferation and apoptosis of RA-FLSs. It was found that curcumin distinctly suppressed the proliferation of RA-FLSs and induced their apoptosis in a dose-dependent manner. In addition, expression of ALOX5 concurrently exhibited a downward trend with the increase of curcumin concentration. The findings suggested that curcumin might play a suppressive role in inflammation in RA via suppressing the expression of ALOX5 protein.

## 5. Conclusions

The current study delves into the potential mechanism of action of curcumin in the treatment of rheumatoid arthritis (RA), employing a multifaceted approach that combines machine learning, network pharmacology, molecular dynamics, and cellular experiments. The findings reveal that ALOX5 plays a pivotal role in RA pathology, and curcumin demonstrates a strong affinity for ALOX5, maintaining stable functionality. Intervention with varying concentrations of curcumin in RA-FLSs led to a decrease in proliferative potential and an increase in apoptosis in a dose-dependent manner. Concurrently, the protein level of ALOX5 showed a downward trend with increasing curcumin concentration.

Consequently, the study suggests that curcumin may exert its therapeutic effects in RA by downregulating the expression of ALOX5, offering a novel ALOX5-targeted therapeutic strategy for RA. However, the exact mechanism of action remains to be elucidated, necessitating further investigation in animal models. Future research could investigate the impact of curcumin on other relevant molecules and signaling pathways involved in the inflammatory process of RA, as well as its long-term efficacy and safety in RA treatment..

## Abbreviations

RA                      Rheumatoid Arthritis

ALOX5	Arachidonate 5-Lipoxygenase
IL-1 $\beta$	Interleukin-1 $\beta$
LTs	Leukotriene
TNF- $\alpha$	Tumor Necrosis Factor - $\alpha$
SVM	Support Vector Machine
RMSD	Root mean Square Deviation
RG	Radius of Gyration
SASA	Solvent-Accessible Surface Area
RA-FLSs	Ra Fibroblast-Like Synoviocytes
DMSO	Dimethyl Sulfoxide
PVDF	Polyvinylidene Fluoride
PBS	Phosphate Buffered Saline
IL-6	Interleukin-6
PUFA	Polyunsaturated Fatty Acids
AA	Arachidonic Acid
LTB4	Leukotriene b4
NF- $\kappa$ B	Nuclear Factor Kappa b

## Ethical Approval

This study did not include any human participants or animals.

## Author Contributions

**Jianwei Xiao:** Conceptualization, Formal Analysis, Writing – original draft

**Xinmin Huang:** Project administration, Visualization

**Xu Cai:** Data curation, Software, Visualization

**Yiwei Hong:** Funding acquisition, Project administration, Validation

**Zhenbo Yan:** Data curation, Formal Analysis, Methodology

**Xinpeng Chen:** Conceptualization, Writing – review & editing

## Funding

The present study was funded by the Chinese Medicine Research Project of Traditional Chinese Medicine Bureau of Guangdong Province (20221342), and the Shenzhen Futian District Health and Public Welfare Research Project (grant no. FTWS2022021, FTWS2022043, FTWS2023027, FTWS2023046).

## Data Availability Statement

The data used in this study were obtained from GEO (<https://www.ncbi.nlm.nih.gov/geo/>).

## Conflict of Interest

The authors declare no conflict of interest.

## References

- [1] Smolen JS, Aletaha D, McInnes IB. Rheumatoid arthritis. *Lancet*. 2016; 388(10055): 2023-2038. [https://doi.org/10.1016/s0140-6736\(16\)30173-8](https://doi.org/10.1016/s0140-6736(16)30173-8)
- [2] McInnes IB, Schett G. The pathogenesis of rheumatoid arthritis. *N Engl J Med*. 2011; 365(23): 2205-2219. <https://doi.org/10.1056/nejmra1004965>
- [3] Gheorghe KR, Korotkova M, Catrina AI, et al. Expression of 5-lipoxygenase and 15-lipoxygenase in rheumatoid arthritis synovium and effects of intraarticular glucocorticoids. *Arthritis Res Ther*. 2009; 11(3): R83. <https://doi.org/10.1186/ar2717>
- [4] Mengli Wu, et al. The role of leukotriene B4 in the pathogenesis of rheumatoid arthritis. *Chinese Journal of Immunology*. 2014, 30(05): 689-693. <https://doi.org/10.3969/j.issn.1000-484X.2014.05.028>
- [5] Smolen JS, van der Heijde D, Machold KP, et al. Proposal for a new nomenclature of disease-modifying antirheumatic drugs [J]. *Ann Rheum Dis*. 2014; 73(1): 3-5. <https://doi.org/10.1136/annrheumdis-2013-204317> PMID: 24072562.
- [6] Kuttan G, Kumar KB, Guruvayoorappan C, et al. Antitumor, anti-invasion, and antimetastatic effects of curcumin. *Adv Exp Med Biol*. 2007; 595: 173-184. [https://doi.org/10.1007/978-0-387-46401-5\\_6](https://doi.org/10.1007/978-0-387-46401-5_6)
- [7] Xiao J, Cai X, Zhou W, et al. Curcumin relieved the rheumatoid arthritis progression via modulating the linc00052/miR-126-5p/PIAS2 axis. *Bioengineered*. 2022; 13(4): 10973-10983. <https://doi.org/10.1080/21655979.2022.2066760>
- [8] Daina A, Michielin O, Zoete V. SwissTargetPrediction: updated data and new features for efficient prediction of protein targets of small molecules. *Nucleic Acids Res*. 2019; 47(W1): W357-W364. <https://doi.org/10.1093/nar/gkz382>
- [9] Keiser MJ, Roth BL, Armbruster BN et al. Relating protein pharmacology by ligand chemistry. *Nat Biotechnol*. 2007; 25(2): 197-206. <https://doi.org/10.1038/nbt1284>
- [10] Jiménez J, Doerr S, Martínez-Rosell G et al. DeepSite: protein-binding site predictor using 3D-convolutional neural networks. *Bioinformatics*. 2017; 33(19): 3036-3042. <https://doi.org/10.1093/bioinformatics/btx350>
- [11] MALDE A K, ZUO L, BREEZE M, et al. An automated force field topology builder (ATB) and repository: Version 1.0. *Journal of Chemical Theory and Computation*, 2011, 7(12): 4026-4037. <https://doi.org/10.1021/ct200196m>
- [12] Kumari R, Kumar R; Open Source Drug Discovery Consortium, Lynn A. g\_mmpbsa--a GROMACS tool for high-throughput MM-PBSA calculations. *J Chem Inf Model*. 2014; 54(7): 1951-1962. <https://doi.org/10.1021/ci500020m>
- [13] Hamzehzadeh L, Atkin SL. The versatile role of curcumin in cancer prevention and treatment. A focus on PI3K/AKT pathway. *J Cell Physiol*. 2018; 233(10): 6530–6537. <https://doi.org/10.1002/jcp.26620>

- [14] Murray-Stewart T, Casero RA. Regulation of polyamine metabolism by curcumin for cancer prevention and therapy. *Med Sci*. 2017; 5(4): E38:38. <https://doi.org/10.3390/medsci5040038>
- [15] Zhang S, Zou J, Li P, et al. Curcumin protects against atherosclerosis in apolipoprotein E-knockout mice by inhibiting toll-like receptor 4 expression. *J Agric Food Chem*. 2018; 66(2): 449–456. <https://doi.org/10.1021/acs.jafc.7b04260>
- [16] Chen M, du ZY, Zheng X, et al. Use of curcumin in diagnosis, prevention, and treatment of Alzheimer's disease. *Neural Regen Res*. 2018; 13(4): 742–752. <https://doi.org/10.4103/1673-5374.230303>
- [17] Zhuyong Li, Liqiang Wen, et al. The effect of curcumin on inhibiting the proliferation of rheumatoid arthritis synovial fibroblasts [J]. *Lingnan Journal of Emergency Medicine*. 2018, 06: 564-566+576. <https://doi.org/10.3969/j.issn.1671-301X.2018.06.019>
- [18] Al-Madol MA, Shaqura M, John T, et al. Comparative Expression Analyses of Pro- versus Anti-Inflammatory Mediators within Synovium of Patients with Joint Trauma, Osteoarthritis, and Rheumatoid Arthritis. *Mediators Inflamm*. 2017; 2017: 9243736. <https://doi.org/10.1155/2017/9243736>
- [19] Rådmark O, Werz O, Steinhilber D, et al. 5-Lipoxygenase, a key enzyme for leukotriene biosynthesis in health and disease. *Biochim Biophys Acta*. 2015; 1851(4): 331-339. <https://doi.org/10.1016/j.bbali.2014.08.012>
- [20] Živković NP, Petrovečki M, Lončarić ČT, et al. Positron emission tomography-computed tomography and 4-hydroxynonenal-histidine immunohistochemistry reveal differential onset of lipid peroxidation in primary lung cancer and in pulmonary metastasis of remote malignancies. *Redox Biol*. 2017; 11: 600-605. <https://doi.org/10.1016/j.redox.2017.01.005>
- [21] Berbée JFP, Mol IM, Milne GL, et al. Deuterium-reinforced polyunsaturated fatty acids protect against atherosclerosis by lowering lipid peroxidation and hypercholesterolemia. *Atherosclerosis*. 2017; 264: 100-107. <https://doi.org/10.1016/j.atherosclerosis.2017.06.916>
- [22] Chao H, Liu Y, Fu X, et al. Lowered iPLA2 $\gamma$  activity causes increased mitochondrial lipid peroxidation and mitochondrial dysfunction in a rotenone-induced model of Parkinson's disease. *Exp Neurol*. 2018; 300: 74-86. <https://doi.org/10.1016/j.expneurol.2017.10.031>
- [23] Gaschler MM, Stockwell BR. Lipid peroxidation in cell death. *Biochem Biophys Res Commun*. 2017; 482(3): 419-425. <https://doi.org/10.1016/j.bbrc.2016.10.086>
- [24] Singh NK, Rao GN. Emerging role of 12/15-Lipoxygenase (ALOX15) in human pathologies. *Prog Lipid Res*. 2019; 73: 28-45. <https://doi.org/10.1016/j.plipres.2018.11.001>
- [25] Peters-Golden M, Henderson WR Jr. Leukotrienes. *N Engl J Med*. 2007; 357(18): 1841-1854. <https://doi.org/10.1056/NEJMc073333>
- [26] Gürsel T, Firat S, Ercan ZS. Increased serum leukotriene B4 level in the active stage of rheumatoid arthritis in children. *Prostaglandins Leukot Essent Fatty Acids*. 1997; 56(3): 205-207. [https://doi.org/10.1016/s0952-3278\(97\)90535-4](https://doi.org/10.1016/s0952-3278(97)90535-4)
- [27] Zheng LX, Li KX, Hong FF, Yang SL. Pain and bone damage in rheumatoid arthritis: role of leukotriene B4. *Clin Exp Rheumatol*. 2019; 37(5): 872-878.
- [28] Chen M, Lam BK, Kanaoka Y, et al. Neutrophil-derived leukotriene B4 is required for inflammatory arthritis. *J Exp Med*. 2006; 203(4): 837-842. <https://doi.org/10.1084/jem.20052371>
- [29] Lin HC, Lin TH, Wu MY, et al. 5-Lipoxygenase inhibitors attenuate TNF- $\alpha$ -induced inflammation in human synovial fibroblasts. *PLoS One*. 2014; 9(9): e107890. <https://doi.org/10.1371/journal.pone.0107890>